# A Tide-Generated Internal Waveform in the Western Approaches to the Strait of Gibraltar

**2 authors**, including:

Robert Arnone
University of Southern Mississippi
**277** PUBLICATIONS   **5,560** CITATIONS

**Some of the authors of this publication are also working on these related projects:**

Dynamic anomaly bio-physical hotspots in Gulf of MExico  View project

Maritime Advanced Geospatial Intelligence Craft  View project

# A Tide-Generated Internal Waveform in the Western Approaches to the Strait of Gibraltar

Paul E. La Violette and Robert A. Arnone

*Naval Ocean Research and Development Activity, Stennis Space Center, Mississippi*

Aircraft expendable bathythermograph, radar, infrared scanner, and visual data collected in October 1982, 1984, and 1985, as well as space shuttle photographs, indicate that an internal waveform (depending on flow conditions, either an internal hydraulic jump or a lee wave) is a semipermanent feature over the Camarinal Sill in the western approaches to the Strait of Gibraltar. Comparison of these data with both historic and recent current meter mooring data indicates that the waveform, generated at the interface between the Atlantic and Mediterranean waters, undergoes periodic changes wrought by interaction of the tidal current and the flow of the Atlantic and Mediterranean waters. We believe that the waveform is a major mixing mechanism between the two water masses.

## 1. Introduction

Numerous investigators have noted eastward moving internal waves in the Strait of Gibraltar [e.g., *Jacobson and Thompsen*, 1934; *Frassetto*, 1964; *Zigenbein*, 1970; *Boyce*, 1975; *Lacombe and Richez*, 1982; *La Violette et al.*, 1986]. These studies indicate that the maximum amplitudes of the waves occur at the density interface between the surface, comparatively fresh (salinity of $\sim 36$) Atlantic Water (AW) and the deeper, saltier (salinity of $\sim 38$) Mediterranean Water (MW). The waves are generated in groups or "packets" at or near the Camarinal Sill (Figure 1) in association with the tide.

The subsurface waves cause distinctive surface roughness patterns that are visible from ships and aircraft. Various investigators have suggested that these patterns result from the straining of surface waves by internal vertical movement (see, for example, *Gasparovic et al.* [1985]). The patterns have been observed inside the strait on ship radars [*Frassetto*, 1964; *Zigenbein*, 1969; *Cavanie*, 1972]. *La Violette et al.* [1986] measured the areal extent and movement of the waves at the strait's eastern end using a shore-based radar.

In October 1982 a solitary, stationary internal waveform was repeatedly observed in the immediate area over the Camarinal Sill [*Donde Va? Group*, 1984]. These observations were made visually and by aircraft radar and airborne expendable bathythermograph (AXBT) data. Subsequently, two airborne investigations were made of the solitary wave: the first in October 1984 and the second in October–November 1985.

In this paper we will relate the observations made during these flights to the flow, the bathymetric constrictions, and the tidal current. We will then present a simple descriptive model of a spring tidal cycle to characterize the origin, periodicity, and structure of the internal waveform found at the sill.

## 2. The Regional Bathymetry

The bathymetry of the Strait of Gibraltar and its western approaches (Figure 1) constricts the flow in and out of the Mediterranean Sea. The Strait of Gibraltar (characterized by the Tarifa Narrows cross section in Figure 1) is a narrow, steep-sided trough that is angled 21° north of an easterly direction. The Camarinal and Spartel sills separate this trough from the Atlantic.

The cross sections in Figure 1 display an important aspect of the bathymetry: that the regional flow is both horizontally and vertically constricted. The Camarinal Sill cross-sectional area is smaller ($3.75 \times 10^6$ m$^2$) than the Tarifa Narrows ($5.5 \times 10^6$ m$^2$) or the Spartel Sill ($5.7 \times 10^6$ m$^2$). Note the cross-sectional areas above and below 125 m. Both the Spartel and Camarinal sills have more area above 125 m than in the Tarifa Narrows. Thus surface flow is less restricted at the sills than in the Tarifa Narrows. Below 125 m, both the Tarifa Narrows and Spartel Sill have more area than the Camarinal Sill. Thus below 125 m, flow in the Tarifa Narrows and, to a lesser extent, the Spartal Sill is less constricted than that over the Camarinal Sill.

## 3. The Mean Two-Layer Flow and the East-West Tidal Current Components

The total flow through the region is formed by the addition of (1) the mean two-layer flow (Figure 2) with (2) the semidiurnal tidal current [*Lacombe and Richez*, 1982; *Candela et al.*, 1987] and (3) low-frequency changes (produced mainly by wind and atmospheric pressure changes [see *Crépon*, 1965; *Garret*, 1983]. Although the influences of the wind and atmosphere may be strong at times, they do not consistently dominate the total flow as does the tidal current.
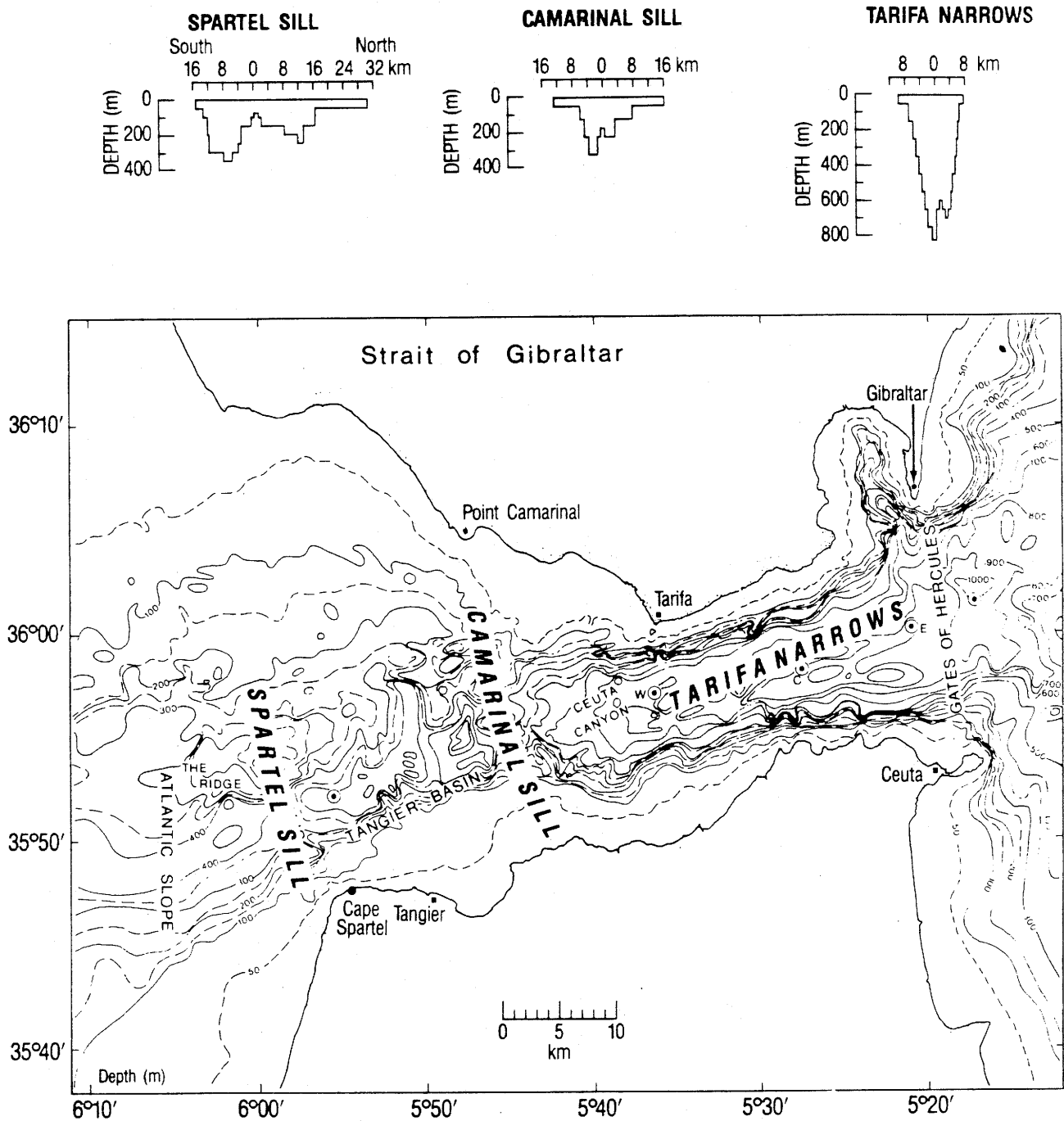
Fig. 1. The bathymetry of the Strait of Gibraltar (modified by *Armi and Farmer* [1985] from *Lacombe and Richez* [1982] and *Giermann* [1961]).

Tidal current variations are closely related to tidal height variations. The tidal height in the strait is predominantly semidiurnal of the form number $F = (K + 0_1)/(M_2 + S_2) = 0.08$ [*DeFant*, 1961] (although tide data show a significant diurnal effect). Maximum tidal currents occur during the periods with the greatest ranges in tide height (i.e., spring), and minimum tidal currents occur during periods with the smallest height ranges (i.e., neap).

*Lacombe and Richez* [1982] indicated that the maximum westward tidal current occurs 3 hours before high water ($-3$ HW) and that the maximum eastward strength occurs 3 hours after high water ($+3$ HW), with essentially no eastward or westward component at either high or low water. Figure 3 shows a smoothed curve of these components' surface strength variations during a tidal cycle at the Camarinal Sill. Based on the *Lacombe and Richez* [1982] data, the curve is a simple
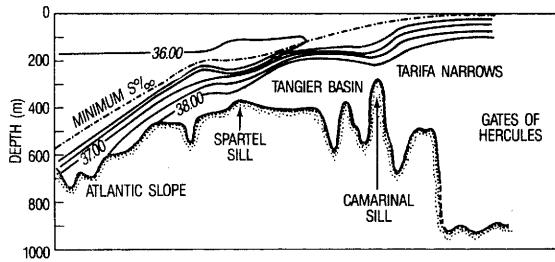
Fig. 2. The mean flow through the Strait of Gibraltar based on 1960 NATO and French ship data. The 37 isohaline separates the fresher Atlantic Water (above) from the saltier Mediterranean Water (below). Going from west to east, the Atlantic Water layer thins and accelerates, while the Mediterranean Water undergoes a similar transformation from east to west [after Lacombe and Richez, 1982].

algebraic addition of hourly current values and then a division of the total to derive the mean eastward flow: 25 cm/s. On a graph of current values versus time, the ordinate was displaced that amount, and the result is the strength and direction of the tidal current components.

The analyses of Lacombe and Richez [1982] (Figure 4) indicate that at the Camarinal Sill, the reduced cross-sectional area combined with the depth decrease results in faster flow than in the other regions and most importantly, causes the flow of both layers to reverse with the tide (i.e., before high water, both layers flow westward; after high water, both layers flow eastward). In addition, their analyses indicate that at the Spartel Sill the flow reverses only in the surface layer (in the deeper layer, the flow is almost always toward the Atlantic). In the Tarifa Narrows the deep layer flow reverses, and the surface flow is almost always toward the Mediterranean.

The analyses by Candela et al. [1987] of long-term current meter mooring data (positioned in 1985 and 1986 as part of the Gibraltar Experiment [see Kinder and Bryden, 1987]) showed that the Lacombe and Richez [1982] analyses of limited data were representative of the tidal currents and the flow interaction. Two 3-day samples of the Candela et al. [1987] analyses for spring and neap tidal conditions at the Camarinal Sill are shown in Figure 5. J. Candela (personal communication, 1988) indicates that the Gibraltar Experiment moorings at the Spartel Sill and in the eastern end of the strait showed the same general reversals as reported by Lacombe and Richez [1982].

This depth-oriented reversing and nonreversing flow at the Spartel Sill and Tarifa Narrows plays an important role in depriving the Camarinal Sill of MW or AW at critical periods of the tide. This role will be discussed in more detail in section 7.

## 4. The Formation of a Hydraulic Jump or a Lee Wave Over the Sill

Farmer and Freeland [1983] showed that internal waveforms that develop, as a result of two-layer flow over sills (i.e., either a hydraulic jump or a lee wave) depend on sill shape,

density stratification, and tidal forcing strength. For example, internal lee waves can maintain their position with respect to the sill only if the flow is subcritical (i.e., they have a composite Froude number for both layers of less than 1).

$$G^2 = F^2_{layer\,1} + F^2_{layer\,2} \qquad (1)$$

The flow is supercritical when $G^2 > 1$, critical when $G^2 = 1$, and subcritical when $G^2 < 1$. Hydraulic control occurs at the crossover point, i.e., the point where the flow is critical. Its location is a function of the channel cross-sectional area, relative density difference, and upstream conditions. If one layer is much deeper than the other, then that layer is essentially passive, and the other layer determines control. In the present study areas this occurs only in the Tarifa Narrows, where the MW layer is much deeper than the AW layer.

In their discussion on mode $i$ internal waves, Farmer and Freeland [1983] state that internal lee waves will occur if the flows upstream and downstream of the sill are both subcritical. A hydraulic jump will occur if the conditions are supercritical upstream of the sill and subcritical downstream. Lee waves are by definition stationary with respect to the bottom (or in this case, the sill). With increasing flow speed, the wave energy propagates away from the sill more slowly, resulting in an accumulation of energy close to the area of generation. This relationship suggests a transformation of a large breaking wave into a train of smaller-amplitude waves or solitons at low flow speed as critical conditions are approached ($F_i$ approaches 1) and as the wave energy becomes concentrated close to the sill (Figure 6).

In studies of internal wave packets in other ocean regions, Osborne and Burch [1980] and Apel et al. [1985] indicate that a hydraulic jump or a large lee wave may form in the immedi-
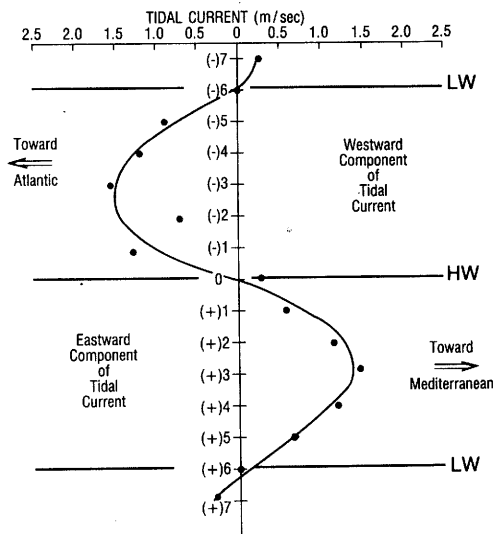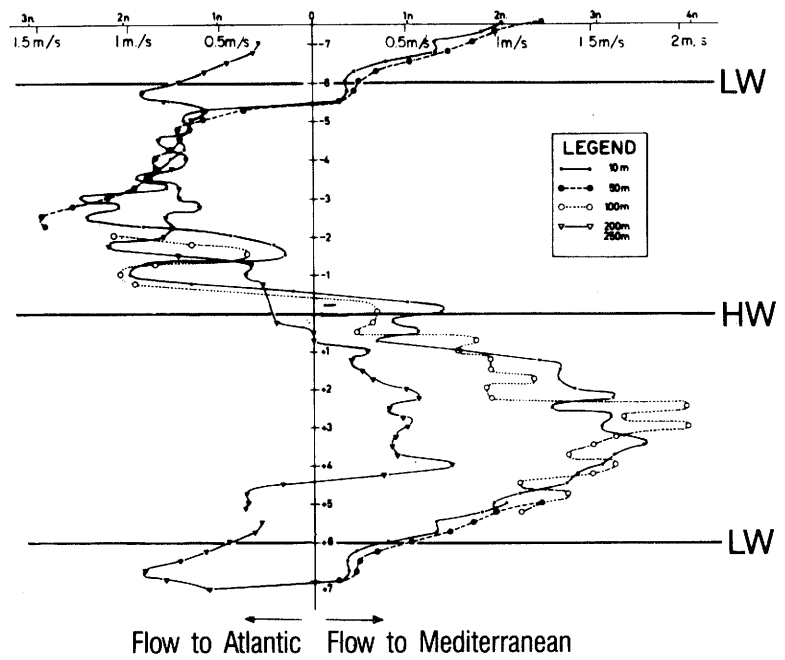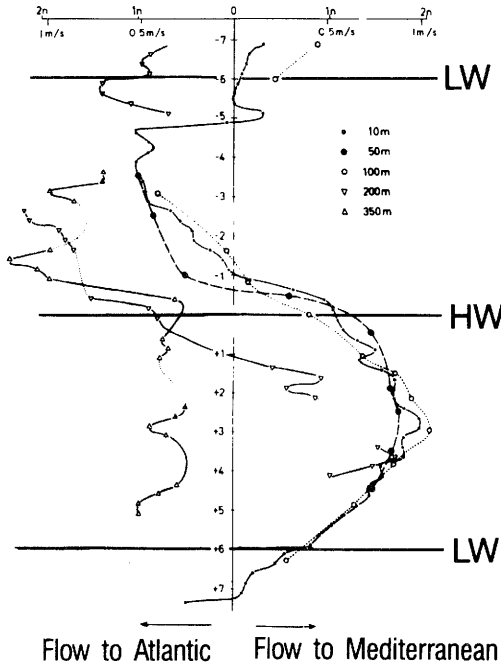


Fig. 3. The west and east components of the surface (10 m) tidal current versus time for the Camarinal Sill (derived from Lacombe and Richez [1982]). Note that a schematic presentation of this curve is included in several of the other figures to indicate the relative strength and direction of the tidal current at the time of the figure.

## SPARTEL SILL (A)
### 18 September 1960



Flow to Atlantic    Flow to Mediterranean

## CAMARINAL SILL (B)
### 25 September 1960



Flow to Atlantic    Flow to Mediterranean

## TARIFA (C)
### 24-25 September 1960



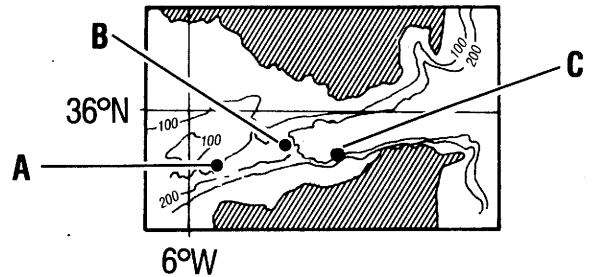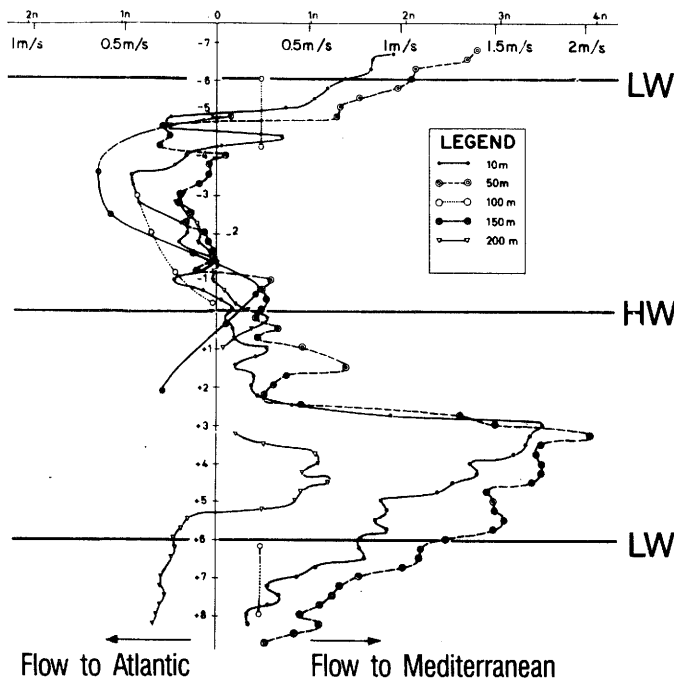Flow to Atlantic              Flow to Mediterranean

Fig. 4.   Current changes at different depths during a 12-hour tidal cycle at three positions in the Strait of Gibraltar and its western approaches. On the graphs each curve relates to a particular depth. On the ordinate, time is represented as plus or minus the hours from high water (HW). On the abscissa, speed is represented in meters per second going east and west from a null center line [after *Lacombe and Richez*, 1982].
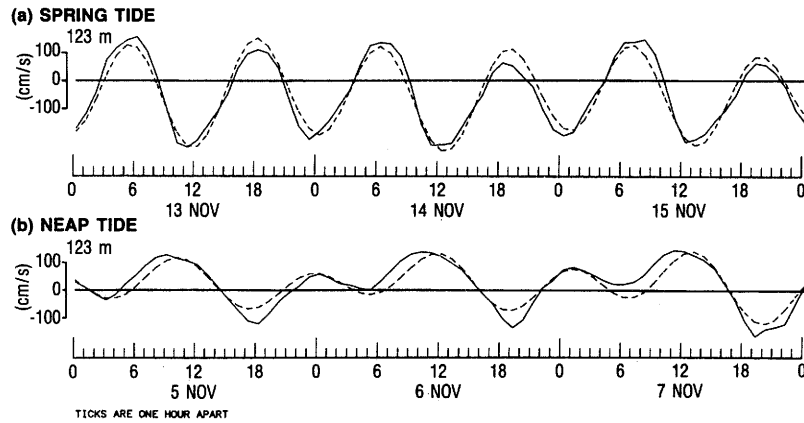
**(a) SPRING TIDE**

123 m



```
0    6    12   18   0    6    12   18   0    6    12   18   0
      13 NOV             14 NOV             15 NOV
```

**(b) NEAP TIDE**

123 m



```
0    6    12   18   0    6    12   18   0    6    12   18   0
      5 NOV              6 NOV              7 NOV
```

TICKS ARE ONE HOUR APART

Fig. 5. Observed (solid lines) and predicted (dashed lines) currents obtained from current meter moorings on the Camarinal Sill (35°58.79'N, 5°44.41'W) for 3-day periods for spring and neap tides. The plots show the total hourly currents (along their principal axis) observed at each depth [*Candela et al.*, 1987].

ate areas of regional bathymetric sills owing to tidal flow. *Armi and Farmer* [1985], in studies of the Strait of Gibraltar, suggested that a hydraulic jump may occur at the Camarinal Sill.

## 5. THE AIRBORNE PLATFORMS AND SPACE SHUTTLE DATA

Two airborne investigations were made: the first in October 1984 and the second in October–November 1985. Observations were also made during 9 strait transit flights in 1982 and 12 in 1986.

In October 1984 the space shuttle *Challenger* (NASA mission STS-41-G) made daily flights at local noon over the strait area. Following directions by the airborne scientists, the shuttle crew took more than 40 photographs of the strait region during October 5 through 12. At that time, the strait was repeatedly overflown at different tidal stages by helicopter and aircraft equipped with 70- and 35-mm cameras, an infrared scanner (uncalibrated), and search radar. On October 8 and 11, helicopter flights monitored the surface roughness patterns for 30 min every 2 hours for most of a tidal cycle (navigation was established by radial bearings and ranges from the Gibraltar airport radar, which gave location accuracies of ±200 m).

The 1985 helicopter flights were made on October 29 (1 day after spring tide) and November 9 (3 days after neap tide). Ship-tide XBTs were deployed during the October 29 flights for three separate stages of a tidal cycle. Each drop session took less than 30 min.

## 6. RESULTS

The XBT data, the airborne visual, infrared scanner, and radar observations, as well as the shuttle photographs, dis-
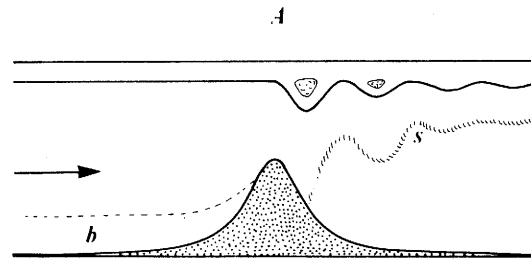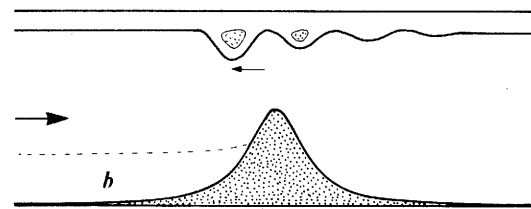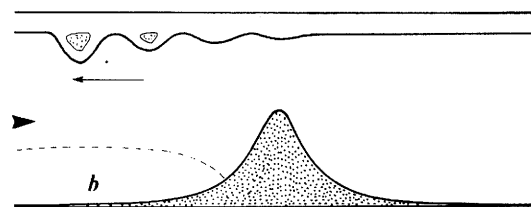


Fig. 6a



Fig. 6b



Fig. 6c

Fig. 6. Schematic diagram of a mode *i* lee wave response to tidally forced flow over a sill. Upstream of the sill there is blocking (b) of the deep flow and separation (s) of the boundary layer beneath the trough of the lee wave downstream of the sill (Figure 6a). As the tidal current slackens (Figures 6b and 6c), the lee waves are released successively to form a nonlinear wave train that travels over the sill crest and back upstream [*Farmer and Freeland*, 1983].
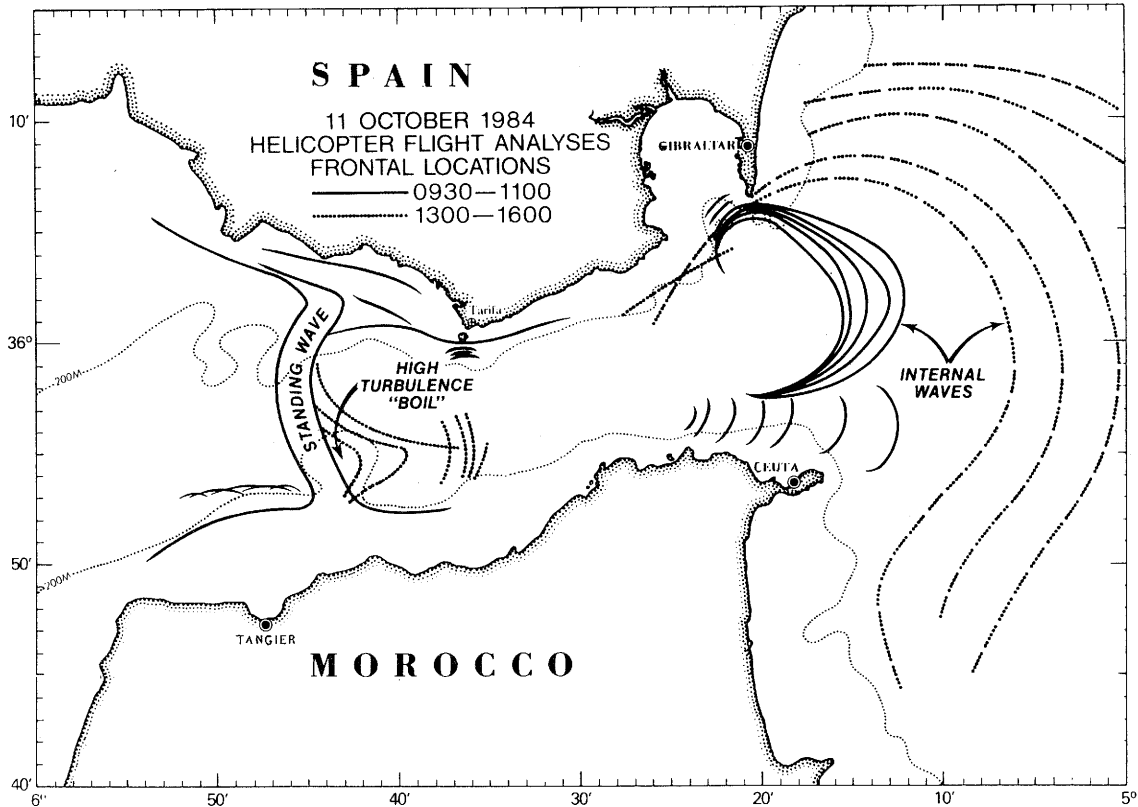
Fig. 7.  Diagram of the positions of the surface roughness features associated with the internal waveforms over the Camarinal Sill and those of the progressive internal waves moving eastward through the strait on October 11, 1984. Note the westward bowing of the double roughness pattern seen over the sill and the high turbulence area just east of the sill. Compare the diagram to the shuttle photograph in Plate 1 that was taken concurrently with the helicopter flight. (From a sketch made aboard the helicopter.)

close that an internal waveform with distinct surface roughness patterns was almost always present over the Camarinal Sill (the exceptions occurred at low tides, especially during neaps). The surface patterns were grossly aligned with the bathymetry of the sill in being bowed westward. The patterns showed east and west fluctuations of approximately 3 to 4 km that coincided with the tidal stage. Figure 7, drawn aboard a helicopter, shows the surface patterns of 1 day's flights.

XBT vertical sections for three stages of a tidal cycle on October 29, 1985, are presented in Figure 8. At $-4$ HW, a hydraulic jump or a lee wave was observed directly over the sill (note that the 16°C isotherm is vertically displaced more than 100 m). The surface temperatures over the sill were cooler than the slightly warmer water to the east. The thermal interface was deepest west of the sill, and the interface isotherms were more broadly spaced. A double line of surface roughness was visible.

At $+2$ HW the isotherms do not show vertical changes as large as those at $-4$ HW (the vertical displacement of the 16°C isotherm is 50 m; slightly east of the sill, the 15°C isotherm is displaced 25 m). The thermal interface was generally weaker and the surface waters over the sill slightly colder (17°C) than at $-4$ HW. A single line of surface roughness was visible. At LW, Figure 8c shows a broad distribution of the isotherms with a comparatively weak interface (the 16°C iso-

therm shows only a gentle eastward rise) and a fairly uniform surface temperature. No diagnostic surface roughness pattern was present.

The October 11, 1984, helicopter flights are an example of the roughness patterns observed over a tidal cycle (Figure 7 was drawn during this day's flights). Figure 9 places this and the next day's flights in temporal context with the tides and the shuttle photographs.

The initial observations at 0830 UT ($-5$ HW) showed a long, well-defined line of rough water aligned with the sill (Figure 10). Two hours later, at 1030 UT ($-3$ HW), the surface pattern had changed to a north-south, 1-km-wide band of water that had the appearance of rapid internal movement but almost no waves. On each side of the band lay a sharp line of rough water. (The October 11 photographs of the band are too poor to reproduce here. However, photographs from other days (e.g., Figure 11) showed this particular roughness pattern more clearly.)

Plate 1 presents one of several space shuttle photographs taken of the study area an hour later ($-2$ HW). (Plate 1 is shown here in black and white. The color version can be found in the separate color section in this issue.) The sunglint in the photograph illuminates both the surface roughness patterns associated with the internal jump/lee wave over the sill and those of internal wave packets spreading eastward from

**STATION LOCATION**

**(a) -4 HW**
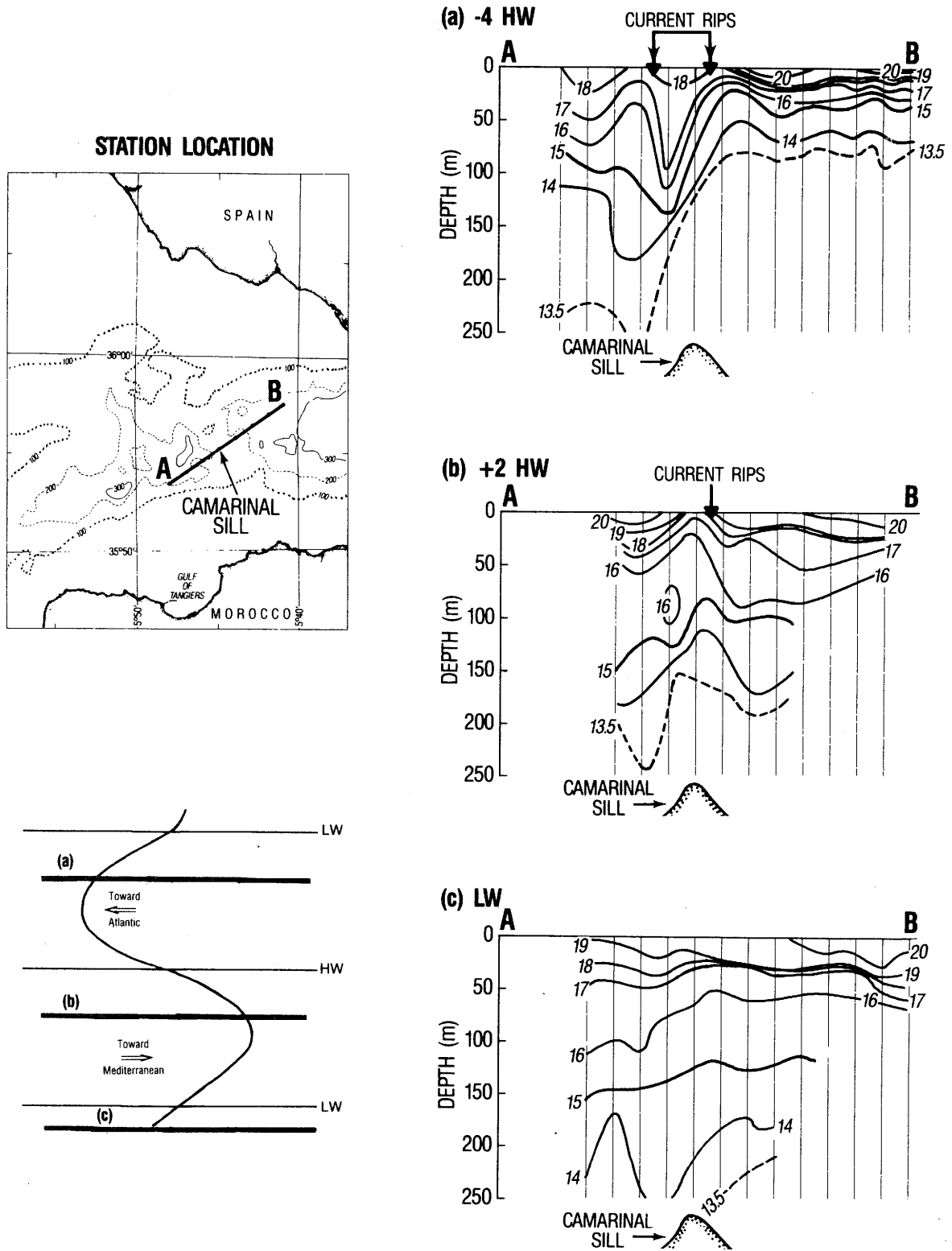
**(b) +2 HW**

**(c) LW**

Fig. 8.   Ship-type XBT cross sections across the Camarinal Sill for (a) 4 hours before high water, (b) 2 hours after high water, and (c) low water on October 29, 1985 (+1 day spring). The thin vertical lines mark the approximate 1-km spacing of the XBT data used in each cross section. The schematic tidal current curve shows the relative strength and direction of the tidal current for each cross section. The internal disposion of the waveform at the time of each section may be found in Figure 12 and its discussion.
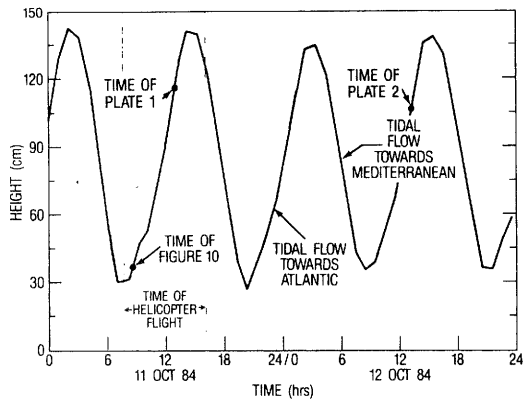
Fig. 9. Diagram showing relation of the heights of the tide (and by inference the tidal current direction) at the time of the helicopter and shuttle photographs shown in Figure 10 and Plates 1 and 2. The inferred disposition of the waveform at the time of each photograph may be found in Figure 12. (Tidal observations furnished by José García-Morán, Instituto Español de Oceanografía, Madrid).

Gibraltar. A shuttle photograph taken at −3.5 HW on the following day (Plate 2) presents clearer details of the surface disturbances over the sill. (Plate 2 is shown here in black and white. The color version can be found in the separate color section in this issue.)

At 1330 UT (HW) a large area of disturbed water had developed in the central portion of the sill. During our 30-min observation period an eastward-bowed band of roughness moved out of the agitated region and moved east toward Tarifa. Similar occurrences were observed during other flights. At 1630 UT (+2 HW) the surface roughness pattern of a small packet of approximately five internal waves was seen proceeding eastward just east of Tarifa. However, at the sill, no distinctive roughness pattern was visible.

Helicopter flights made during a neap tide of October 1985 revealed no distinctive surface patterns over the sill (although roughness patterns indicative of internal wave packets were noted within the strait itself).

## 7. DISCUSSION

### The Model

It would appear that tidal current modulation of the regional flow is the chief cause of the periodic appearance of the waveform over the Camarinal Sill. Using a simple descriptive model of a spring tidal cycle, we can explain the events we believe occurred during our observations (we will try to avoid difficulties by considering the flow and the tidal coefficient to have been the same during all our observations).

Figure 12a shows that the mean flow above 125 m at the Camarinal Sill is composed of eastward moving AW; below 125 m the mean flow is westward moving MW. The dashed line in this and following cross sections in Figure 12 represents the mean depth of the interface of AW and MW. The heavy line in each schematic tidal current curve will indicate the

tidal stage and direction and strength of the tidal current component.

A strong westward tidal current (Figures 3 and 4), the vertical structure shown by XBT data (Figure 8), and the surface roughness patterns (e.g., Figure 9) are characteristic of −4 HW over the sill (Figure 12b). Our model indicates that the westward tidal current both increases the outflow of MW flow and reverses the AW flow.

Two things occur at this time to cause the interface to rise above 125 m. (1) Note that in Figures 4a and 4c the flow of AW at the Spartel Sill reversed, but at Tarifa, AW still flowed into the Mediterranean. This AW divergence results in a decreased volume of AW over the sill (this by itself causes the interface to rise). (2) Note in Figure 4c the increased flow of MW in the Tarifa Narrows due the western tidal current. The result is a buildup of MW east of the sill as the increased volume of MW tries to pass over the sill through the narrow passage below 125 m.

With the decrease in AW over the sill and a buildup of MW east of the sill, the interface rises well above 125 m. MW is now much higher over the sill than directly west of the sill. This increased height increases the flow, and a hydraulic jump or a lee wave forms on the western side of the sill. The diagram shows that at the surface, a north-south line of roughness appears on the western side of the sill, marking the position of the sursurface jump/lee wave.

At −3 HW (Figure 12c) the effect of the westward component of the tidal current is maximum over the sill (Figures and 5). Our model indicates (1) that with maximum volume o MW and minimal volume of AW present over the sill the interface will be closest to the surface and (2) that the height differential with the MW directly west of the sill will be greatest, and a hydraulic jump will form.

Figure 12c shows that a second line of surface roughness becomes evident as the western portion the hydraulic jump nears the surface. Between the two lines is an area of rolling water (Figure 11). As was stated earlier, this surface feature occurs commonly at this time of the tide. The turbulence resulting from the jump or lee wave will produce strong mixing between the outgoing MW and the AW. We believe this is important, as it would mean that AW is significantly modified prior to crossing the Camarinal Sill.

At about −1 HW the westward current component relaxes, and by HW (Figure 12d), events will have changed dramatically over the sill (Figure 6 of Farmer and Freeland [1983] indicates what may be occurring at this time). Our model shows that the waveform west of the sill collapses and that AW now flows eastward over the sill to form nonlinear internal waves that move eastward toward the strait. The strength and number of the internal waves are correlated to the amplitude of the originating wave and indirectly to tide height, such that more and stronger waves are formed during periods of higher tidal amplitudes.

At +3 HW (Figure 12e) the eastward tidal current reaches maximum strength. Less MW flows over the sill owing to a reverse flow in the Tarifa Narrows and a continued westward flow at the Spartel Sill (Figure 4). Our model shows the waveform on the eastern side of the sill to be a lee wave (due to the small differential in height of the interface west of the sill (Figure 8)). At the surface a north-south line delineates the position of the wave.

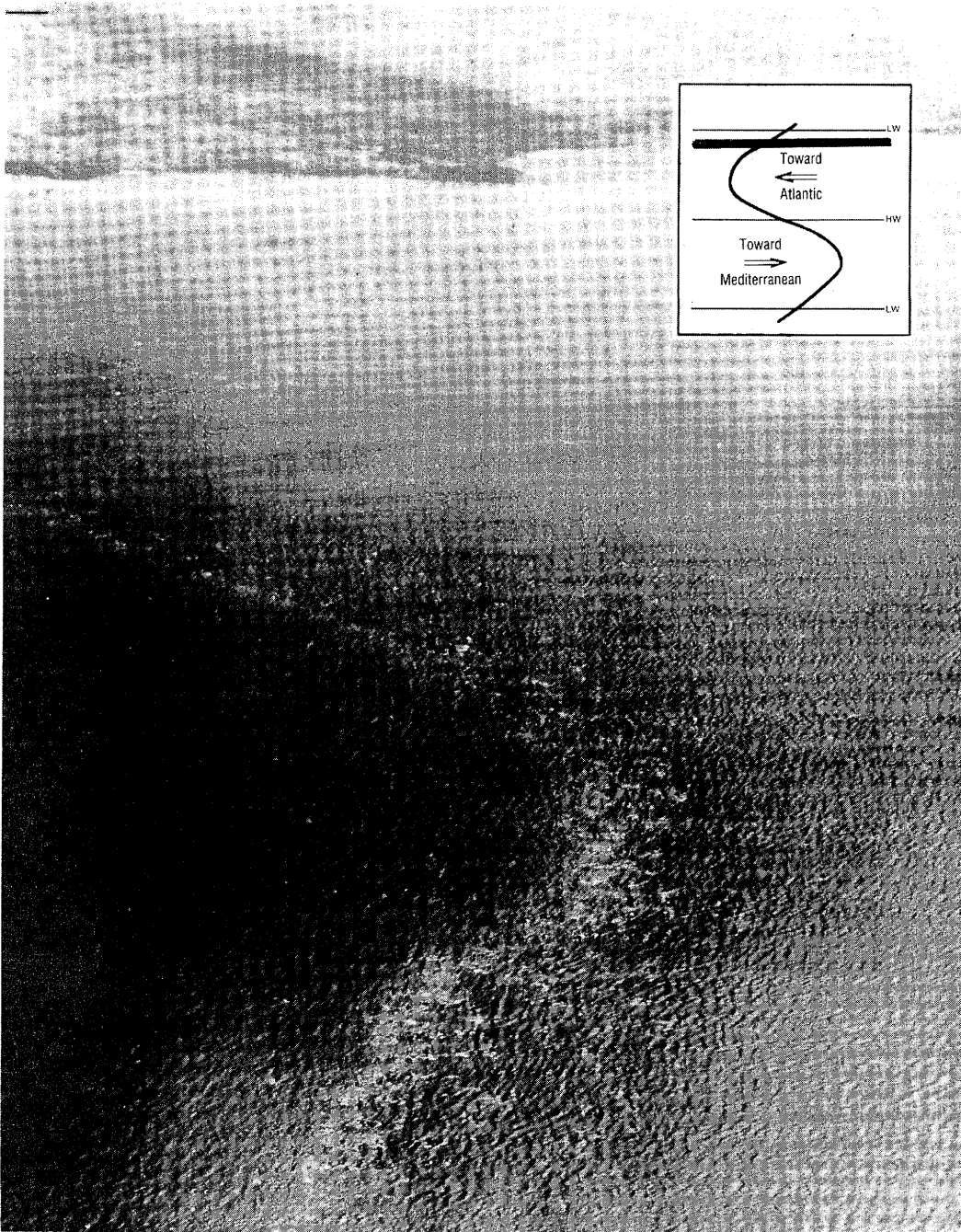At LW (Figure 12f) the situation is unlike that at HW,

Fig. 10. The surface roughness pattern over the Camarinal Sill on October 11, 1984, at 0030 UT (or −4 HW). The schematic shows the relative strength and direction of the tidal current. The subsurface conditions at this time are comparable to those in Figure 12b. (Photograph taken from a helicopter at an altitude of about 700 m looking south toward the Gulf of Tangiers.)

when a resurgent AW rapidly reestablishes itself in the sill area. The reverse flow of MW has gradually been decreasing since shortly after +3 HW, when the eastward tidal current begins to weaken. Flow cross the Camarinal Sill now resembles the mean flow. With the east-west tidal current components at a null position, currents at all depths will approach mean flow conditions.

*Spring and Neap Influence*

As is indicated in the *Candela et al.* [1987] data (Figure 5), the increased tidal amplitudes will result in increased tidal current velocities that will add to or subtract from the general flow. The conditions portrayed in our model will change accordingly. During and near spring tides the turbulent con-
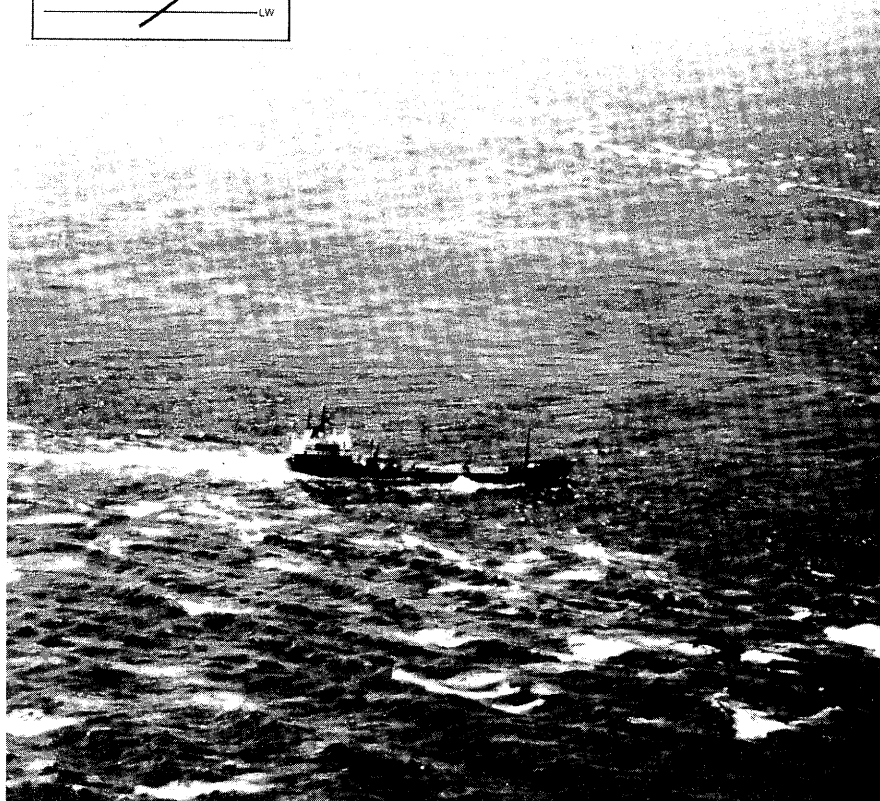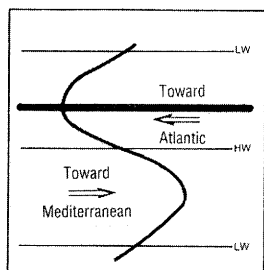
Fig. 11.   The surface roughness pattern over the Camarinal Sill on October 8, 1984, at UT or −3 HW (taken from a helicopter at an altitude of about 300 m looking east toward Tarifa with an 15-m/s easterly wind. The subsurface conditions at this time are comparable to those described in Figures 8a and 12c). The ship entering the central band of rolling water had lost its heading moments earlier and heeled over so that a large wave went over the afterbridge. The ship had no difficulty prior to that time and did not appear to encounter any further difficulty in the central band. This phenomenon was noticed to occur with several other ships about the same period and had been noted on other flights. It has also been reported by mariners traversing the immediate area [e.g., Marine Observer, 1938, 1948, 1951].

ditions that occur between −4 HW and HW will be strongest and will occupy longer periods of the tidal cycle (the roughness patterns shown in the shuttle photographs and the strong local currents will occur during these periods). During and near neap tides the diminished tidal current will have a weak effect on the flow. The result will be that the low tide flow regime will last longer and the structure of the waveform will be minimal.

As is suggested in the model, strong mixing between AW and MW may occur west of the sill prior to HW. If this hypothesis is correct, then it is this highly modified AW that will pass over the sill during the post-HW period. The strongest mixing will always occur during spring. Thus during neaps (1) AW comparatively unmixed with MW will enter the strait, (2) MW entering the Atlantic will be the least mixed

with AW, and (3) the density interface in the strait will be the strongest of the lunar period.

## 8.   CONCLUSIONS

We have presented a simple descriptive model of a spring tidal cycle based on a synthesis of various observations. We believe the data, while comparatively sparse for such a complex area, allow a reasonable analysis of conditions.

The study also illustrates the advantage for ocean study of aircraft and shuttle photographs containing sun glint. The information, while qualitative, can define the distribution of features that have had limited area-scale measurements. Thus as an indicator of the range and distribution of various oceanic phenomena, such photography can be an excellent oceanographic tool.
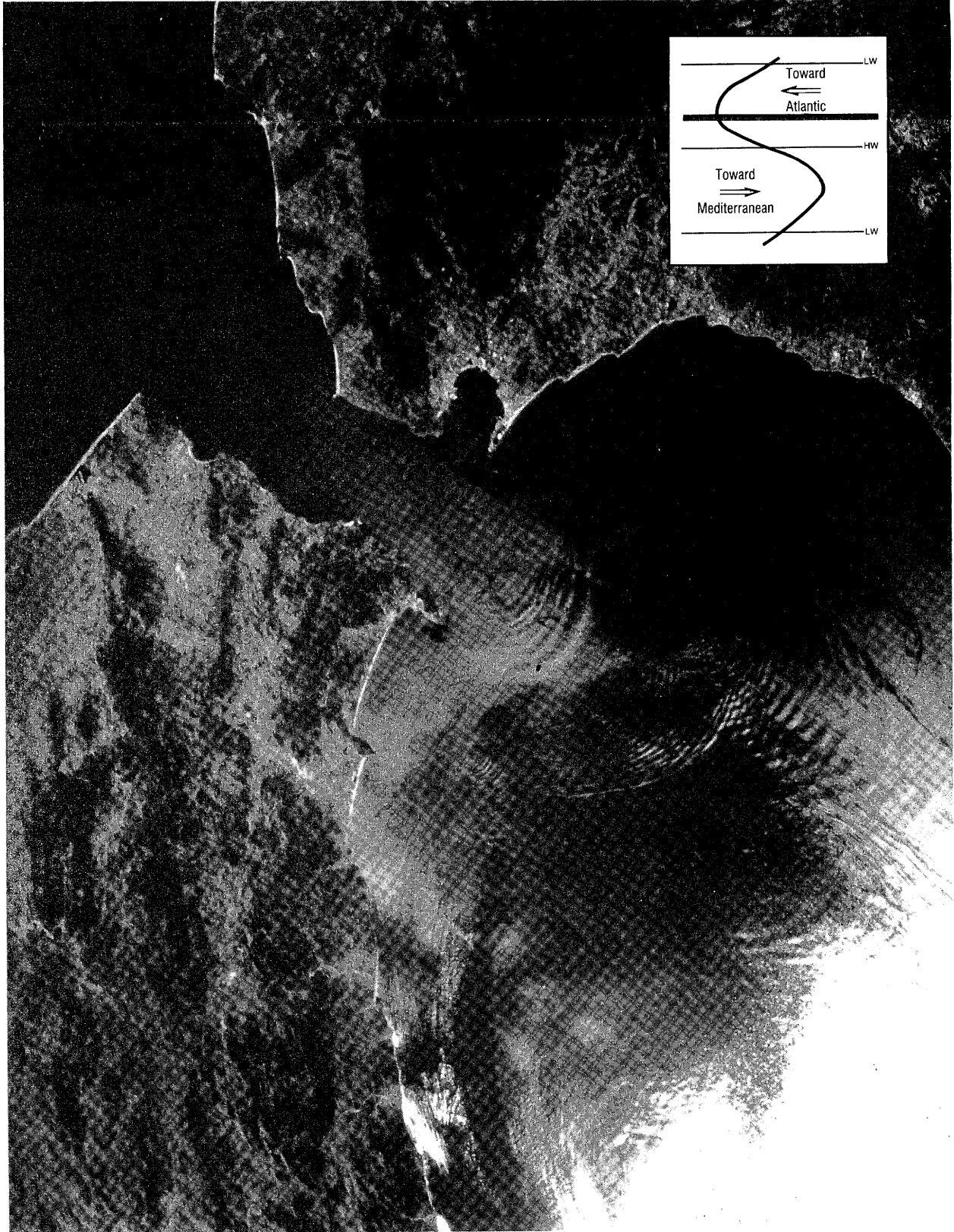
Plate 1. The Strait of Gibraltar and its approaches taken from ~200 km by the shuttle *Challenger* (NASA mission STS 41 G) at 1721 UT, October 11, 1985 (−2 HW, 1.3 days after spring), at the time of the helicopter flight of Figure 7. In the reflection of the noon on the water's varying roughness, a packet of 10 or more internal waves to the right of the strait can be seen moving east into the Mediterranean; the regular spacing indicates their tidal origin. The more subdued area of reflection at the western end of the strait is that of the waveform discussed in this study; subsurface conditions are comparable to a period between Figures 12c and 12d. The internal waves (and all ocean roughness patterns shown) have very small surface amplitude, and brighter reflections come from disturbed (hence more reflective) water. (NASA photograph 34-081). (The color version of this figure can be found in the separate color section in this issue.
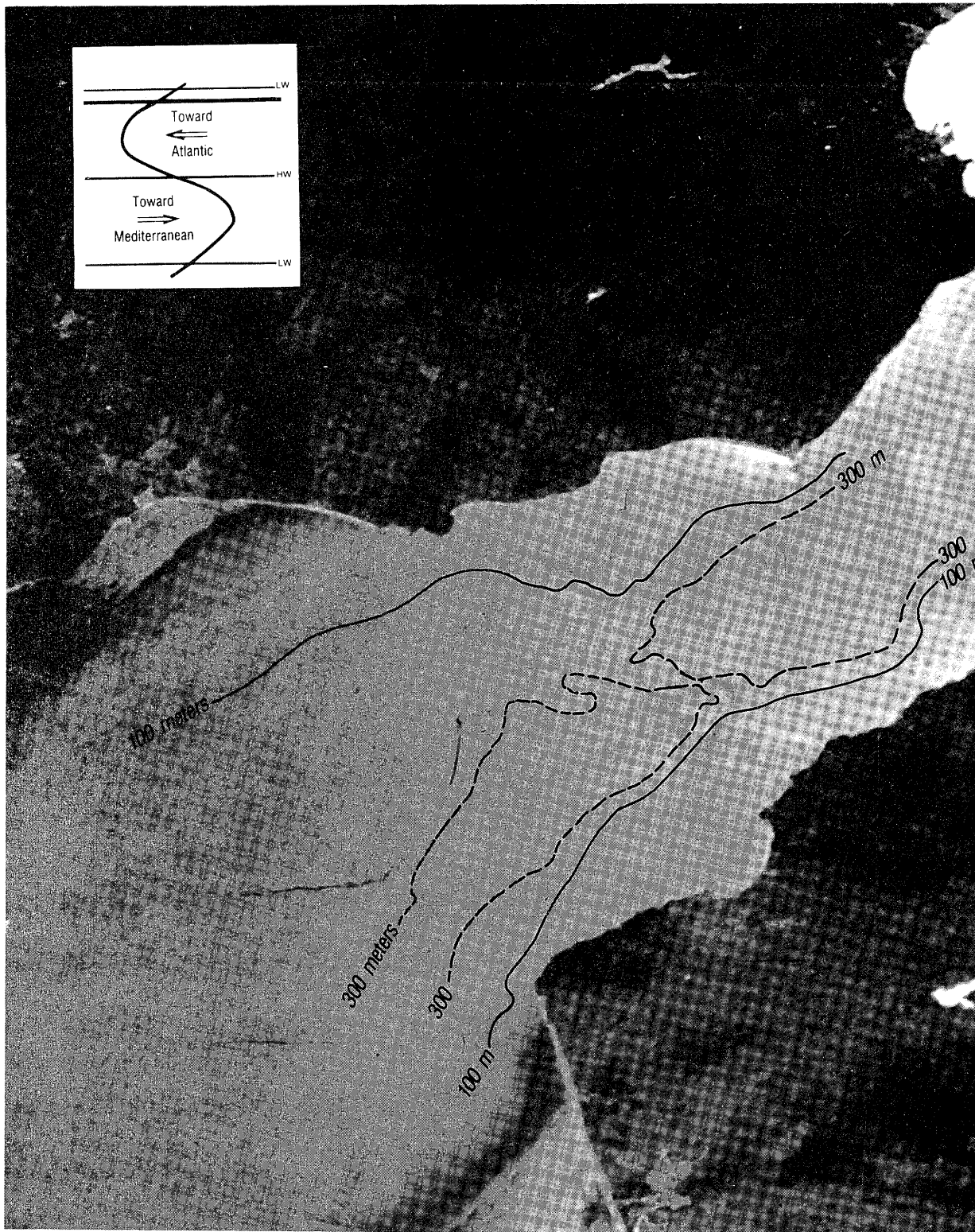
Plate 2. Enlargement of part of a shuttle photograph shows the western approaches to the Strait of Gibraltar from an altitude of 198 km on October 12, 1984, at about 1200 UT (−3.5 HW, 2.5 days after spring). The subsurface conditions at this time are comparable to a period between Figures 12b and 12c. The 100- and 300-m isobaths are presented to show the location of the waveform relative to the Camarinal Sill. Further bathymetric information can be inferred by comparing these isobaths to the chart in Figure 1. (NASA photograph 40-049.) (The color version of this figure can be found in the separate color section in this issue.)
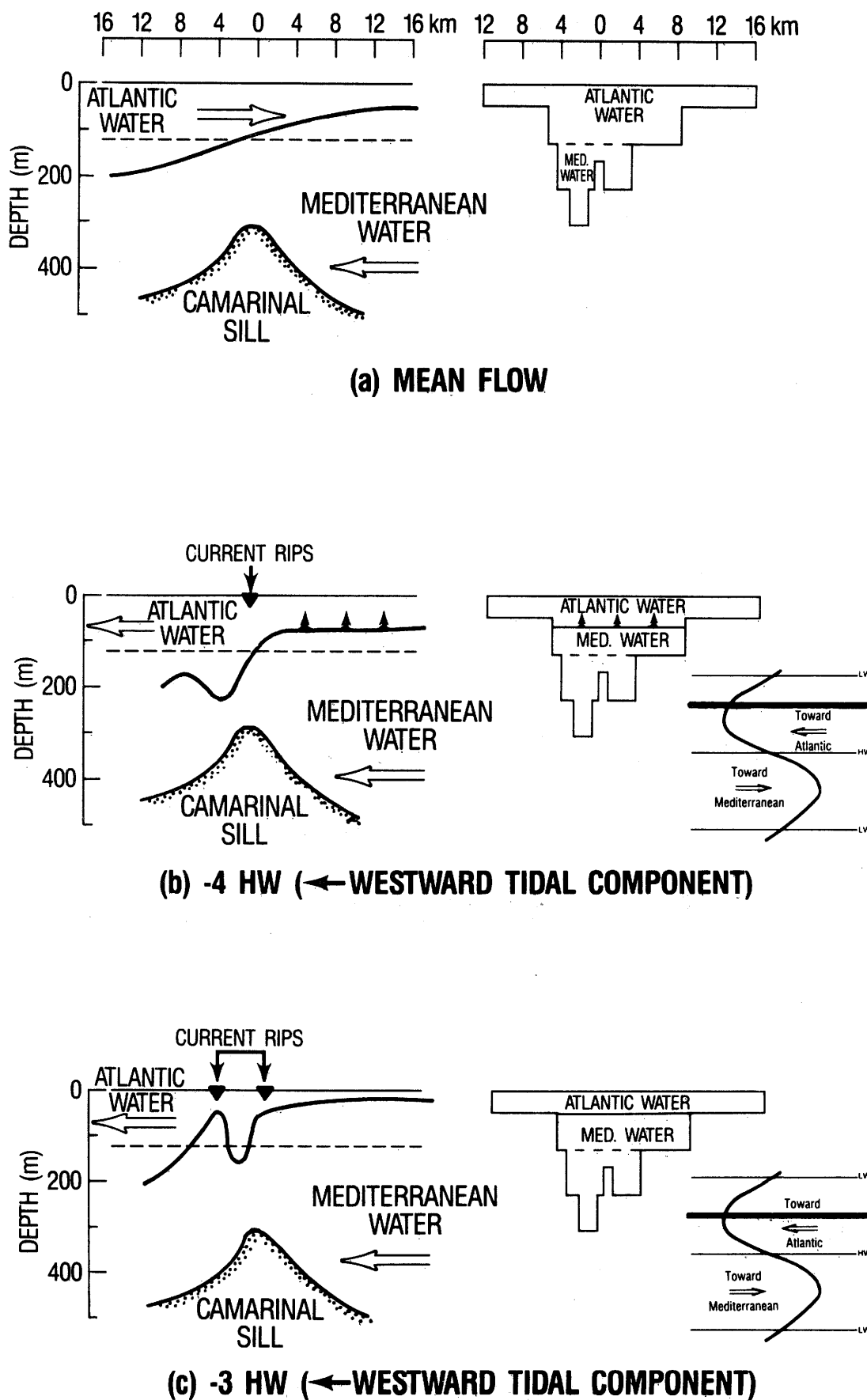
(a) MEAN FLOW



(b) -4 HW (◄─WESTWARD TIDAL COMPONENT)



(c) -3 HW (◄─WESTWARD TIDAL COMPONENT)

Fig. 12. A schematic model of the flow over the Camarinal Sill for different periods of a spring tide: (a) mean flow, (b) −4 HW, (c) −3 HW, (d) HW, (e) +3 HW, and (f) LW.
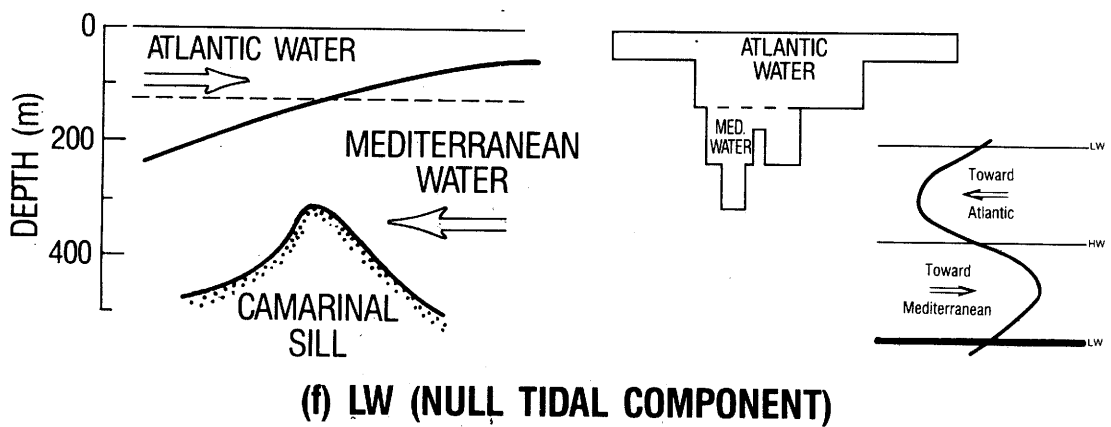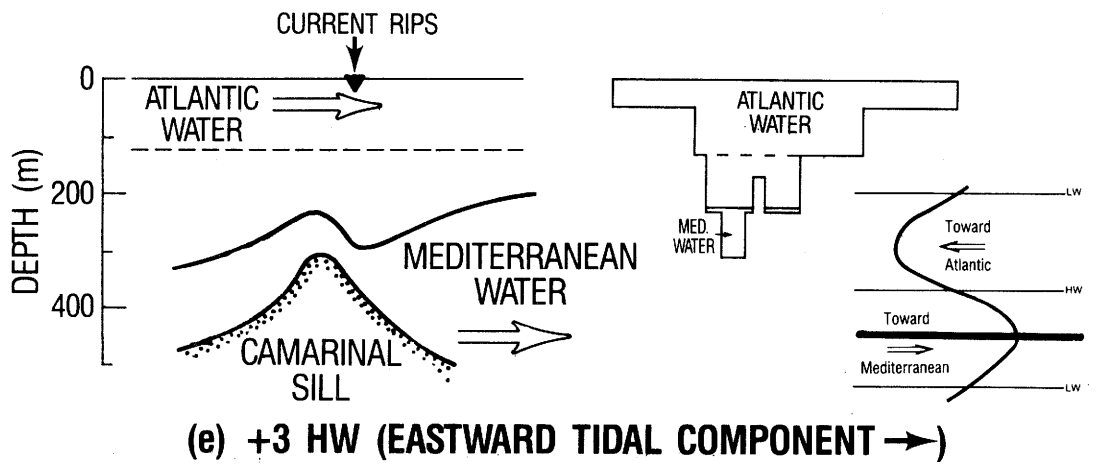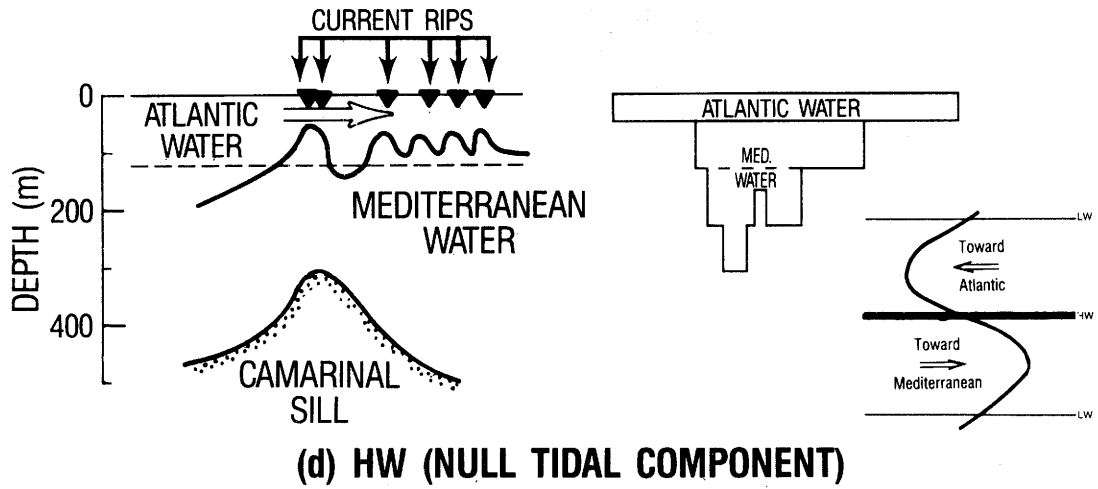
**(d) HW (NULL TIDAL COMPONENT)**



**(e) +3 HW (EASTWARD TIDAL COMPONENT →)**



**(f) LW (NULL TIDAL COMPONENT)**

Fig. 12. (continued)

## REFERENCES

Apel, J. R., J. R. Holbrook, A. K. Liu, and J. J. Tsai, The Sulu Sea internal soliton experiment, *J. Phys. Oceanogr.*, *15*, 1625–1651, 1985.

Armi, L., and D. Farmer, The internal hydraulics of the Strait of Gibraltar and associated sills and narrows, *Oceanol. Acta*, *8*(1), 37–46, 1985.

Boyce, F. M., Internal waves in the Strait of Gibraltar, *Deep Sea Res.*, *22*, 597–610, 1975.

Candela, J., C. D. Winant, and H. Bryden, Observations of the baroclinic tide in the Strait of Gibraltar (abstract), *Eos Trans. AGU*, *68*(50), 1709, 1987.

Cavanie, A. G., Observations de fronts internes dans le Détroit de Gibraltar pendant la campagne oceanographique OTAN 1970 et interpretation des resultats par un modèle mathématique, *Mem. Soc. Sci Liege*, *6*, 27–41, 1972.

Crépon, M. Influence de la pression atmosphérique sur le niveau moyen de la Méditerranée occidentale et sur le flux à travers le détroit de Gibraltar, Présentation d'observations, *Cah. Oceanogr.*, *17*, 14–32, 1965.

DeFant, A., *Physical Oceanography*, vol. II, p. 393, Pergamon, Elmsford, N. J., 1961.

Donde Va? Group, Donde Va?: An oceanographic experiment in the Alboran Sea, *Eos Trans. AGU*, *63*(36), 682–683, 1984.

Farmer, D. M., and H. J. Freeland, The physical oceanography of fjords, *Prog. Oceanogr.*, *12*, 147–219, 1983.

Frassetto, R., Short period vertical displacements of the upper layer of the Strait of Gibraltar, *Tech. Rep. 30*, 49 pp., SACLANT ASW Res. Centre, La Spezia, Italy, 1964.

Garrett, C. J. R., Variable sea level and strait flows in the Mediterranean: A theoretical study of the response to meteorological forcing, *Oceanol. Acta*, *6*, 79–87, 1983.

Gasparovic, R. F., J. R. Apel, A. Brandt, and E. S. Kasischke, Synthetic aperture radar imaging of internal waves, *APL Tech. Dig.*, *6*(4), 338–345, 1985.

Giermann, G., Erlauter ungen zur bathymetrichen Karte der Strasse von Gibralter, *Bull. Inst. Oceanogr.*, *1218A*, 1961.

Jacobsen, J. P., and H. Thompsen, Periodical variations in temperature and salinity in the Strait of Gibraltar, in *James Johnstone Memorial Volume*, pp. 275–293, Liverpool University Press, Liverpool, England, 1934.

Kinder, T. H., and H. L. Bryden, The 1985–1986 Gibraltar Experiment: Data collection and preliminary results, *Eos Trans. AGU*, *68*, 786–795, 1987.

Lacombe, H., and C. Richez, The regime of the Strait of Gibraltar, in *The Hydrodynamics of Semi-Enclosed Seas*, edited by J. C. J. Nihoul, pp. 13–73, Elsevier, Amsterdam, 1982.

La Violette, P. E., and H. Lacombe, Tidal-induced pulses in the flow through the Strait of Gibraltar, *Oceanol. Acta*, in press, 1988.

La Violette, P. E., T. H. Kinder, and D. W. Green III, Measurements of internal waves in the Strait of Gibraltar using a shore-based radar, *Tech. Rep. 118*, 13 pp., Nav. Ocean Res. and Develop Activ., Natl. Space Technol. Lab., Miss., 1986.

*Mar. Observ.*, *15*, 87, 1938.

*Mar. Observ.*, *18*, 138–139, 1948.

*Mar. Observ.*, *21*, 155, 1951.

Osborne, A. R., and T. L. Burch, Internal solitons in the Andaman Sea, *Science*, *208*, 451–460, 1980.

Zigenbein, J., Short internal waves in the Strait of Gibraltar, *Deep Sea Res.*, *16*, 479–487, 1969.

Zigenbein, J., Spatial observations of short internal waves in the Strait of Gibraltar, *Deep Sea Res.*, *17*, 867–875, 1970.

R. A. Arnone and P. E. La Violette, Naval Ocean Research and Development Activity, Stennis Space Center, MS 39529.